

Comparative analysis of accelerating power input and speed input robust power system stabilizers

Javeed Kittur*, Saikumar H V** and Sharath Raj S V**

The power system stability improvement by a robust Power System Stabilizer (PSS) using accelerating power and speed as inputs is investigated independently in this paper. The objective of the work presented in this paper is to design an accelerating power input robust PSS and a speed input robust PSS to damp low frequency oscillations arising out of small and large disturbances. The robustness of the PSS is ensured by placing all the eigen values within a specified contour in the s-plane. A nonlinear constrained optimization technique has been applied for tuning the PSS parameters with the objective of damping oscillations over a wide range of operating conditions to make the PSS robust. The design of PSS is validated by performing nonlinear simulations for small and large disturbances.

Keywords: *D-stability, parameter optimization, power system stabilizer, robust controller, supplementary modulation controller*

1.0 INTRODUCTION

Whenever an AC interconnected power system is subjected to large load variations the system frequency will be severely disturbed. As a consequence the system may tend to become oscillatory [1]. To stabilize the resulting low frequency oscillations in the traditional technique is to install a PSS in the excitation system of the generator. The objective of the PSS is to improve the stability limits on a power transfer by enhancing damping of system oscillations via generator excitation control [2]. Poorly damped oscillations can limit the power transfer under weak system conditions, thus the stabilizer performance must be satisfactory for a wide range of system operating conditions [3].

The concept of stabilizing the synchronous machines through excitation controls using supplementary signals has been discussed in literature [2],[3],[4]. Generally used inputs to the

stabilizer are speed, power and frequency. The ideal variable to be used as a stabilizing signal is rotor speed because the speed signal is in phase with damping torque. PSS has the ability to damp low frequency oscillations and improve overall damping.

The speed signal is inherently sensitive to presence of torsional oscillations at a frequency in the range of 8-20 Hz. This can lead to negative damping of the torsional mode. Speed signal leads to negative damping of intra-plant modes if PSS is not designed effectively. The frequency signal is insensitive to intra-plant modes [5]. If an electric power is used as stabilizing signal, it is subjected to temporary depression in the voltage during the periods of increase in generation and hence accelerating power signal is preferred [4]. The difficulty of measuring rotor speed as well as the need to process such measurement through considerable lead functions to overcome the lags in the excitation system make it more desirable

*B. V. Bhoomaraddi College of Engineering and Technology, Hubli – 580 031, India. Email: javedkittur89@gmail.com

**The National Institute of Engineering, Mysore – 570 008, India. E-mail: sharathmark@yahoo.com

to derive the stabilizing action from acceleration or accelerating power [4]. True accelerating power requires measurement of electrical as well as mechanical power. The measurement of mechanical power is difficult and does not exhibit significant variation for power angle variations. So the mechanical power is derived in a simpler manner using electrical quantities. This approach is discussed by de Mello, Hannet and Undrill [4].

Due to variations in generation and load patterns there is large variation in the small signal dynamic behavior of the system and this can be expressed as a parametric uncertainty. The tuning problem is to choose a set of controller parameters such that the system is well damped for all the parametric uncertainties. The design of PSS deals with choosing a nominal operating condition and then optimizing its performance using nonlinear constrained optimization technique about this operating point. The optimization of the PSS parameters leads to improvement in the damping and system performance. A similar approach is discussed by Shrikant Rao and Indraneel Sen [6]. A logical approach is to first specify the acceptable range of performance and then attempt to obtain a PSS which achieves this specification over the required range of operating conditions.

2.0 PERFORMANCE REQUIREMENTS OF POWER SYSTEM STABILIZER

In power systems, a damping ratio ζ of around 10 to 20% for the low-frequency modes is satisfactory. In addition, if the real parts of the poles α are restricted to be not greater than a specified value, the oscillations will die down within a reasonable time. In the work presented in this paper, the value of ζ and α are chosen as 20% and -0.5 for speed input PSS and ζ and α are chosen as 15% and -0.5 for accelerating power input PSS. For an acceptable performance the closed-loop poles must satisfy these two requirements simultaneously. The frequency of oscillations is related to the synchronizing torque of the generators and hence care should be taken to ensure that the imaginary part of the rotor mode eigenvalue does not fall appreciably due to the feedback [7]. Any controller satisfying these

constraints on the closed-loop rotor mode eigenvalue is acceptable. The new modes resulting from the controller loop must also be stable and well-damped. Finally, a small-loop gain is desirable to avoid possible controller saturation and poor large disturbance response.

If the PSS places all the closed-loop poles to the left of the “D” contour shown in Figure 1, then the specified requirements are satisfied. This property is

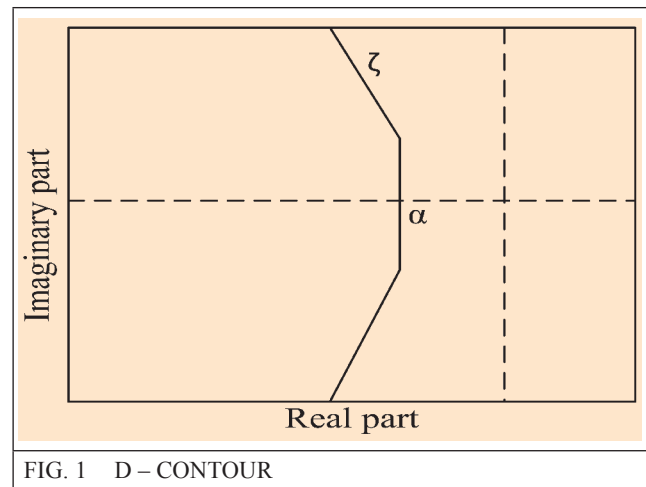


FIG. 1 D – CONTOUR

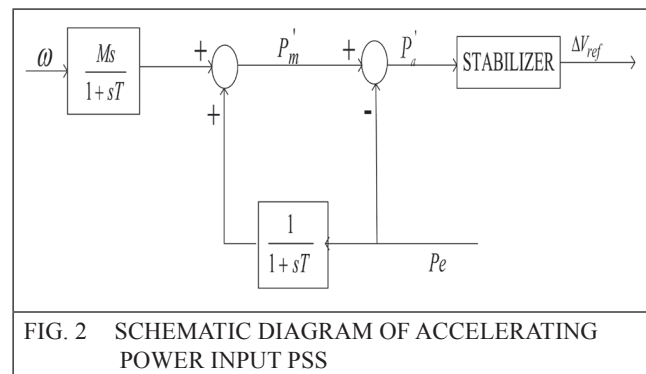


FIG. 2 SCHEMATIC DIAGRAM OF ACCELERATING POWER INPUT PSS

referred to as “D-stability”. Any controller that achieves D–stability for a given wide range of operating conditions is said to be robust, that is, it guarantees an acceptable performance over that range of operating conditions [7].

The complexity in designing such a PSS lies with the parametric uncertainty range of the system. In power systems the model uncertainties are generally large, and most robust controller design methods fail to provide a solution as they incorporate a conservative description of

the uncertainty. Many of the recently developed robust control theories also suffer from this drawback. Frequency domain techniques, such as H-infinity optimization and μ -synthesis do not provide much control over the closed-loop pole location and hence the transient response of the system [7]. On the other hand, the considered approach does not introduce any conservativeness in the uncertainty description and is therefore more likely to provide a solution with acceptable system performance [7].

3.0 ACCELERATING POWER INPUT POWER SYSTEM STABILIZER

The accelerating power input PSS uses electrical power and derived measurement of mechanical power as shown in Figure 2.

$$P'_m = \frac{P_m}{1+sT} = \frac{P_e + sM\omega}{1+sT} \quad \dots(1)$$

$$P'_a = P'_m - P_e \approx P_m - P_e \quad \dots(2)$$

where, P'_m is derived mechanical power, P'_a is the derived accelerating power, P_e is the electrical power of generator, $M=2H$ and H is inertia constant, ω is the rotor speed, T is filter time constant ($T=0.005\text{sec}$). The accelerating signal results in minimum lead compensation requirements [5]. The derived signal is insensitive to torsional modes hence torsional filters are ignored. It can be inferred from Figure 2 that the mechanical power P'_m is obtained from electrical power processed through a filter with time constant T and rate of change of speed is also processed with same filter time constant. The advantages of this scheme are discussed by de Mello, Hannet and Undrill [4]. The PSS structure considered in our study is a single stage lead-lag network given below,

$$T(s) = K_{pss} \frac{[1+sT_1]}{[1+sT_2]} \quad \dots(3)$$

where, K_{pss} is the stabilizer gain, T_1 and T_2 are the time constants and these three variables are considered as tunable parameters.

4.0 SPEED INPUT POWER SYSTEM STABILIZER

Among various types of PSS structures, the speed-based lead-lag type PSS is preferred because of the following reasons [8]

- The speed signal is in phase with damping torque.
- Ease of tuning PSS parameters
- Simple in operation and is highly reliable.

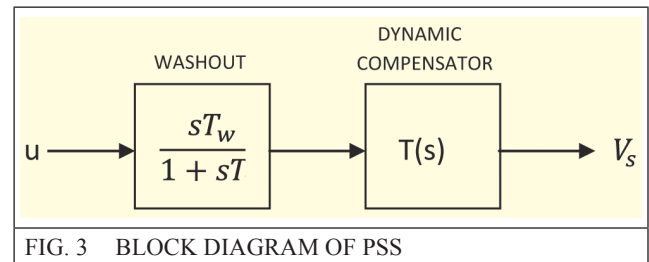


FIG. 3 BLOCK DIAGRAM OF PSS

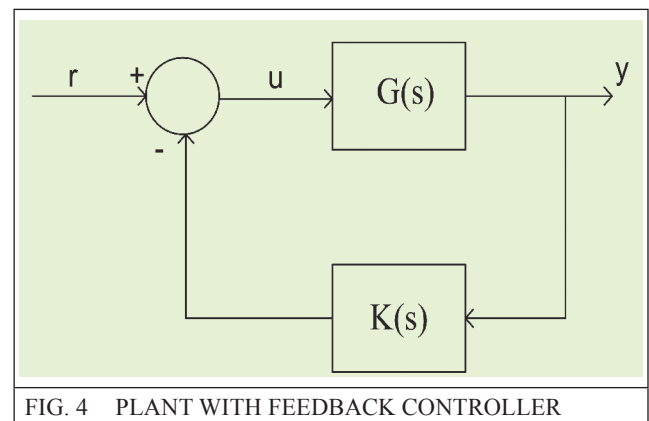


FIG. 4 PLANT WITH FEEDBACK CONTROLLER

The block diagram of PSS is shown in Figure 3. It consists of a washout circuit and a dynamic compensator.

The washout circuit is provided to eliminate the steady state bias in the output of PSS which will modify the generator terminal voltage. The washout circuit acts essentially as a high pass filter and it must pass all frequencies that are of interest. If only the local modes are of interest, the time constant T_w can be chosen in the range 1 to 2. If inter area modes are also to be damped, then T_w must be chosen in the range of 10 to 20. It has been shown that a value of $T_w = 10$ is necessary to improve damping of inter area modes [8]. The dynamic compensator used in this work presented

is a single lead lag stage and it has the transfer function as given by Eq. 3.

5.0 SMALL SIGNAL STABILITY ANALYSIS BY PLANT TEMPLATE

In this paper the focus is only on achieving robust D-stable controller and it is tested at a set of discrete frequencies. Consider the configuration shown in Figure 4, where $G(s)$ is the plant, due to the uncertainty in the plant parameters, $G(s)$ belong to a set, S , of plants. The value set $G(j\omega_i)$, $G \in S$, $\omega_i \in R$, is called the ‘plant template’ at frequency ω_i [7]. A template thus represents the range of variations in the plant response at a particular frequency ω_i . A plant template is plotted on the Nichols chart at any desired frequency by computing $G(j\omega)$ as G varies over the set S and then manually constructing a boundary around the set of obtained points. The introduction of the controller $K(s)$ in the feedback loop, shifts the template at each frequency to a new location on the Nichols chart without transforming its shape. This shift depends upon the value of $K(s)$ at that frequency. The closed loop will be robustly stable, if the controller accompanies the following three criteria [7].

- The templates of the compensated plant ($K(s)G(s)$) do not contain the critical point $(-180^\circ, 0dB)$ on the Nichols chart for all $\omega_i \in R$.
- The set S is connected.
- The nominal closed loop is stable.

Any controller that satisfies the above three conditions robustly stabilizes the given connected set of plants. Figure 5 shows a plant template at 6.5 rad/sec at its original location without PSS and Figure 6 shows the plant template at 6.5 rad/sec but shifted in location after the introduction of the PSS. Each point on this plot represents a computed value of $G(s)$ as G is varied over the set S . The boundary of the template is approximated by straight line segments and is drawn manually. In Figure 5 the plant template encloses the critical point and hence the system is unstable and in Figure 6 the template does not include the critical point thus making the PSS robust.

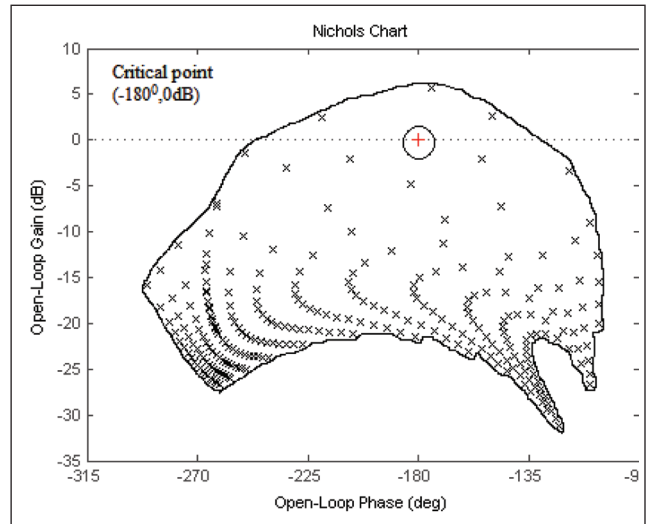


FIG. 5 PLANT TEMPLATE AT $\omega = 6.5 \text{ RAD/SEC}$ WITHOUT PSS

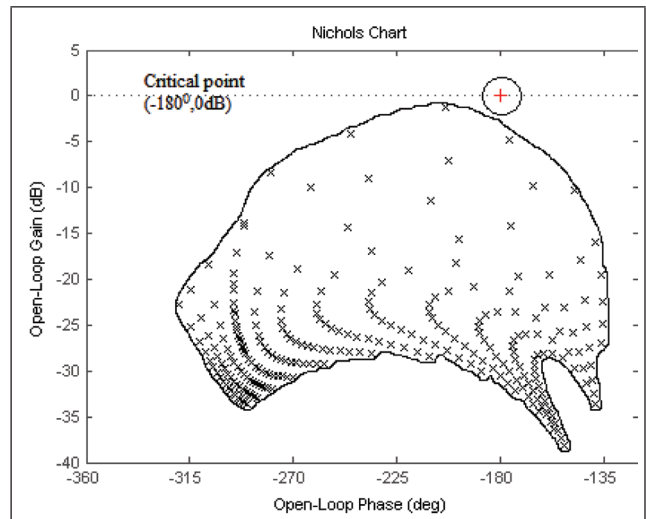


FIG. 6 PLANT TEMPLATE AT $\omega = 6.5 \text{ RAD/SEC}$ WITH PSS

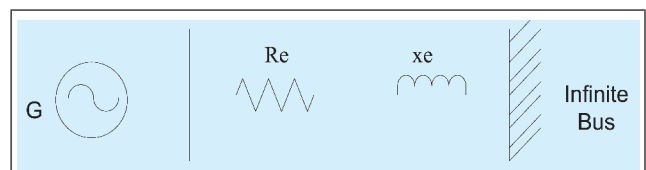


FIG. 7 SINGLE MACHINE INFINITE BUS SYSTEM

6.0 POWER SYSTEM MODEL

Aschematic representation of a SMIB system with a generator connected to an infinite bus by a transmission line is shown in Figure 7. The generator is fitted with an Automatic Voltage Regulator (AVR) and a static excitation system. Neglecting stator transients and the effects of the damper windings, the generator can be modeled

as a fourth order system. The possible variations in operating conditions for this example include variations in the real and reactive powers being supplied by the generator. For the design example for accelerating power input PSS, the real power, P, is assumed to vary from 0.5 to 1.2 pu and the reactive power, Q, from 0 to 0.65 pu and transmission line reactance, x_e , from 0.2 to 0.7 pu. For speed input PSS, the real power, P, is assumed to vary from 0.5 to 1.2 pu and the reactive power, Q, from 0 to 0.65 pu. The transmission line reactance, x_e , from 0.2 to 0.7 pu and the line resistance is neglected. Figure 8 and Figure 9 show the plant poles for the above set of operating conditions without accelerating input PSS and speed input PSS. As seen, most of the operating conditions do not exhibit desirable pole locations.

7.0 CONTROLLER TUNING

A PSS fulfilling the specified requirements of D-stability is obtained by first choosing a particular structure of the PSS, and then solving an optimization problem to compute the parameters. The tunable parameters of the PSS are the controller gain K_{pss} and time constants T_1 and T_2 . The simultaneous tuning of these parameters of PSS has been performed by applying the nonlinear constrained optimization method [9].

The optimization problem is defined as

$$\min \sum_{i=1}^m w_i \alpha_i \quad \dots(4)$$

subject to

$$g_1 \leq \max(\text{Real}(\lambda_i)) - \alpha \quad \dots(5)$$

$$g_2 \leq \zeta - \text{Damp}(\lambda_i) \quad \dots(6)$$

where,

m = total number of modes of interest, α_i = real part of the i^{th} eigenvalue, w_i = weight associated with the i^{th} inter area mode, λ_i are the poles of the nominal plant with controller. $\text{Real}(\)$ represents the real part and $\text{Damp}(\)$ the damping factor of the argument. Constraints $g_1, g_2 < 0$ ensure that the

nominal closed loop is D-stable. The problem now reduces to that of finding a controller such that $g_1, g_2 < 0$. The vector of controller parameters for PSS is therefore given by $[K_{pss} T_1 T_2]^T$.

8.0 IMPLEMENTATION AND RESULTS

The PSS tuning problem is solved by implementing the nonlinear constrained optimization function available in Matlab optimization tool box [9] in the power system simulation program. The optimized controller parameters of accelerating power input PSS are $K_{pss}=2.7271, T_1=0.2225$ and $T_2=1.643$. The optimized controller parameters of speed input PSS are $K_{pss}=17, T_1=0.05$ and $T_2=0.02$. Figure 10 and Figure 11 show the closed loop poles for the set S of plants fitted with accelerating power input PSS and speed input PSS.

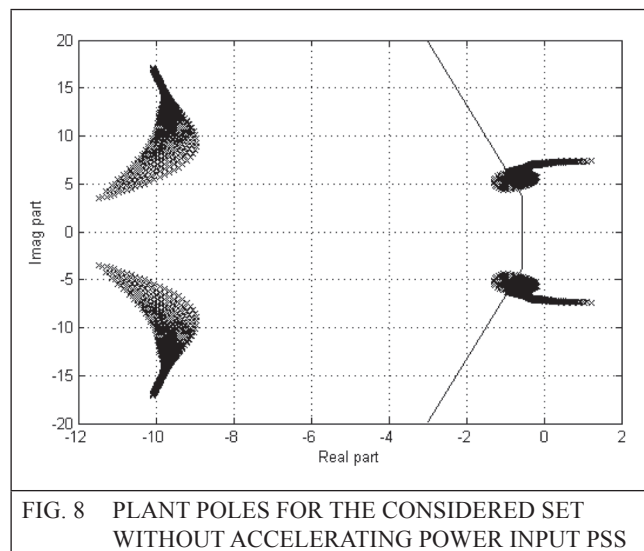


FIG. 8 PLANT POLES FOR THE CONSIDERED SET WITHOUT ACCELERATING POWER INPUT PSS

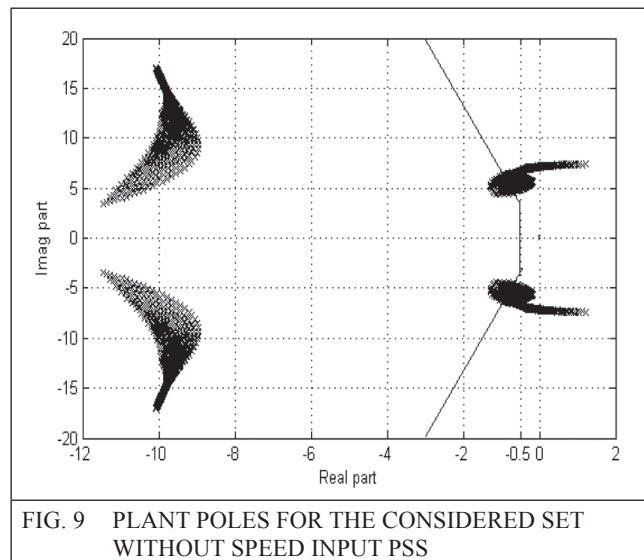


FIG. 9 PLANT POLES FOR THE CONSIDERED SET WITHOUT SPEED INPUT PSS

P and Q have been varied with a step size of 0.05 over the specified range. As can be seen from the eigenvalue plot the closed-loop poles for the entire set lie in an acceptable region, to the left of the D-contour, guaranteeing a well damped system response over the chosen range of operating conditions. Table 1, Table 2, Table 3, Table 4, Table 5 and Table 6 show the eigenvalues for different operating system conditions with accelerating power input PSS and speed input PSS. As stated in the requirements for a robust controller the damping factor should be greater than 15% and 20% and the real part of the eigenvalue should be less than -0.5 for accelerating power input PSS and speed input PSS, these conditions are attained as shown in tables.

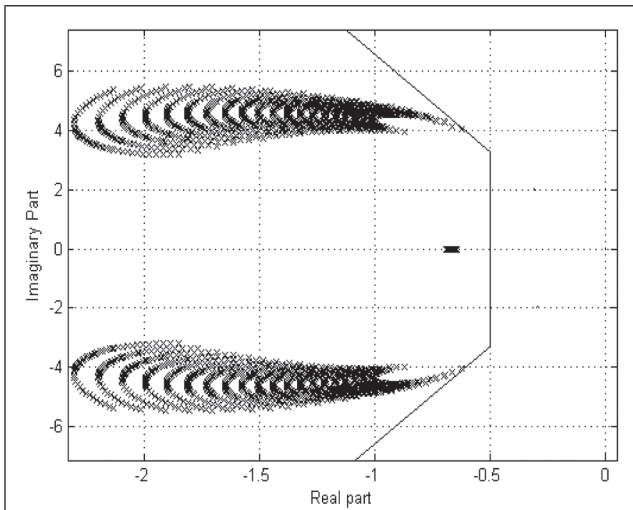


FIG. 10 CLOSED LOOP PLANT POLES WITH ACCELERATING POWER INPUT PSS

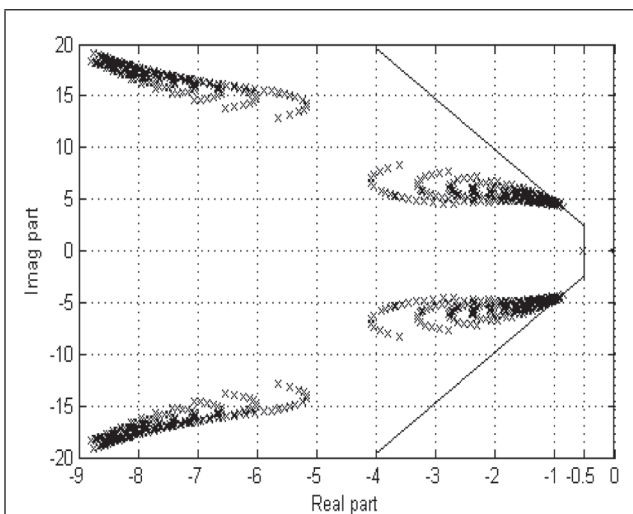


FIG. 11 CLOSED LOOP PLANT POLES WITH SPEED INPUT PSS

TABLE 1			
EIGEN VALUES WITH AND WITHOUT PSS (P=1.2PU, Q=0.65PU AND X _E =0.7PU)			
Without PSS		With Pa input PSS	
<i>Eigen values</i>	<i>Damping Ratio</i>	<i>Eigen values</i>	<i>Damping Ratio</i>
0.66463 + 5.637i	-0.11709	-202.53	1
0.66463- 5.637i	-0.11709	-8.1452 + 21.593i	0.35294
-10.853+15.301i	0.57852	-8.1452 - 21.593i	0.35294
-10.853-15.301i	0.57852	-0.7584 + 4.3972i	0.16998
		-0.7584 - 4.3972i	0.16998
		-0.64612	1

TABLE 2			
EIGEN VALUES WITH AND WITHOUT PSS (P=0.5PU, Q=0.05PU AND X _E =0.2PU)			
Without PSS		With Pa input PSS	
<i>Eigen values</i>	<i>Damping Ratio</i>	<i>Eigen values</i>	<i>Damping Ratio</i>
-0.1512+5.5406i	0.02728	-202.68	1
-0.1512-5.5406i	0.02728	-7.5309 + 21.58i	0.32949
-10.08+14.381i	0.57398	-7.5309 - 21.58i	0.32949
-10.08-14.381i	0.57398	-1.3399 + 3.8532i	0.32845
		-1.3399 - 3.8532i	0.32845
		-0.65815	1

TABLE 3			
EIGEN VALUES WITH AND WITHOUT PSS (P=1.0PU, Q=0.2087PU AND X _E =0.4PU)			
Without PSS		With Pa input PSS	
<i>Eigen values</i>	<i>Damping Ratio</i>	<i>Eigen values</i>	<i>Damping Ratio</i>
0.5090+ 7.1561i	-0.0709	-203.47	1
0.5090 - 7.1561i	-0.0709	-6.8251+ 21.946i	0.29697
-10.741+ 12.104i	0.66373	-6.8251 - 21.946i	0.29697
-10.741- 12.104i	0.66373	-1.6508 +4.5562i	0.34065
		-1.6508 - 4.5562i	0.34065
		-0.65364	1

TABLE 4			
EIGEN VALUES WITH AND WITHOUT PSS (P=1.0PU, Q=0.2087PU AND X _E =0.4PU)			
Without PSS		With Pa input PSS	
<i>Eigen values</i>	<i>Damping Ratio</i>	<i>Eigen values</i>	<i>Damping Ratio</i>
-10.7405+12.1037i	0.6637	-51.2478	1
-10.7405 -12.1037i	0.6637	-0.5320	1
0.5091 + 7.1561i	-0.0710	-4.7072 + 7.4180i	0.5358
0.5091 - 7.1561i	-0.0710	-4.7072 - 7.4180i	0.5358
		-4.8844 +11.6732i	0.3860
		-4.8844 -11.6732i	0.3860

TABLE 5			
EIGEN VALUES WITH AND WITHOUT PSS ($P=0.5\text{PU}, Q=0.05\text{PU}$ AND $X_E=0.2\text{PU}$)			
Without PSS		With Pa input PSS	
Eigen values	Damping Ratio	Eigen values	Damping Ratio
-0.4595 + 5.9395i	0.0771	-51.2459	1
-0.4595 - 5.9395i	0.0771	-3.8718 + 12.5212i	0.2954
-9.8290 + 10.5223i	0.6826	-3.8718 - 12.5212i	0.2954
-9.8290 - 10.5223i	0.6826	-0.5671	1
		-5.7603 + 1.9159i	0.9489
		-5.7603 - 1.9159i	0.9489

TABLE 6			
EIGEN VALUES WITH AND WITHOUT PSS ($P=1.2\text{PU}, Q=0.65\text{PU}$ AND $X_E=0.7\text{PU}$)			
Without PSS		With Pa input PSS	
Eigen values	Damping Ratio	Eigen values	Damping Ratio
-10.965 + 14.2227i	0.6106	-51.0003	1
-10.965 - 14.2227i	0.6106	-8.1226 + 13.9964i	0.5019
0.7661 + 6.4585i	-0.1178	-8.1226 - 13.9964i	0.5019
0.7661 - 6.4585i	-0.1178	-0.5247	1
		-1.5642 + 6.7988i	0.2242
		-1.5642 - 6.7988i	0.2242

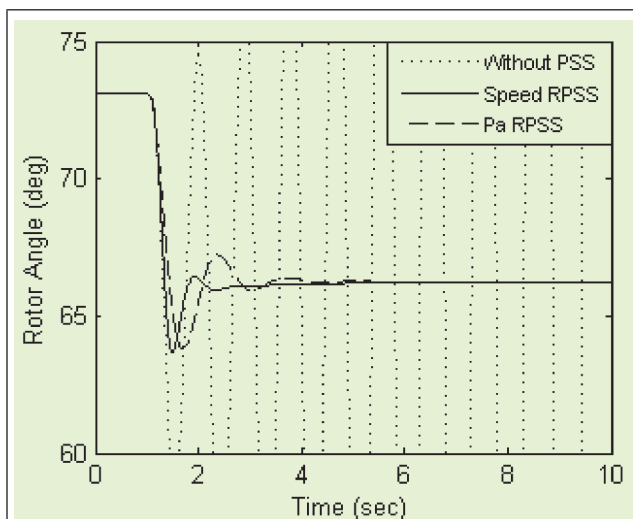


FIG. 12 VARIATION OF ROTOR ANGLE FOR SMALL DISTURBANCE ($P=1.0\text{PU}, Q=0.2087\text{PU}, X_E=0.4\text{PU}$)

The performance of the controller is evaluated by analyzing the system response to a small and large disturbance at various operating conditions with and without controller. In small signal analysis a 5% step change in the reference voltage is considered. Figure 12 and Figure 13

show the variation in the rotor angle and power at generator bus for small perturbation with system nominal operating condition $P=1.0\text{ pu}, Q=0.2087\text{ pu}$ and $x_e=0.4\text{ pu}$. Figure 14 shows the variation in modulating signal for both types of PSS for small disturbance.

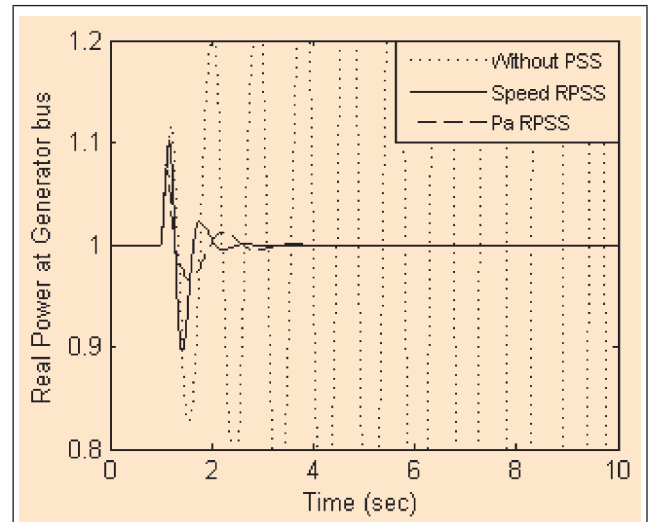


FIG. 13 VARIATION IN REAL POWER AT GENERATOR BUS FOR SMALL DISTURBANCE ($P=1.0\text{PU}, Q=0.2087\text{PU}, X_E=0.4\text{PU}$)

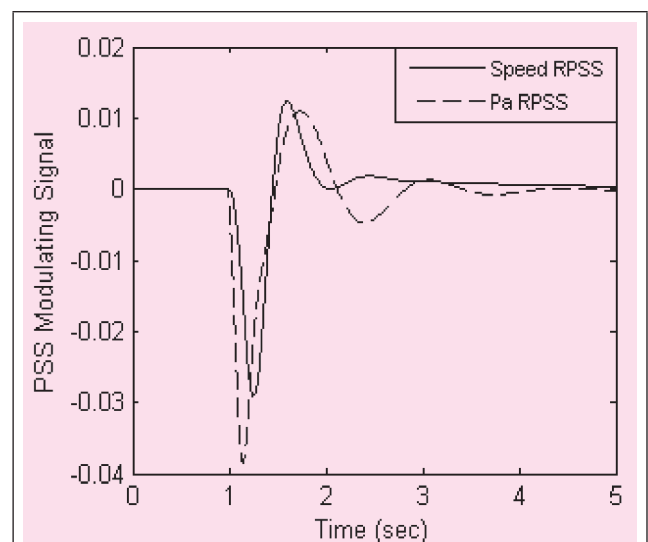


FIG. 14 PSS MODULATING SIGNAL FOR SMALL DISTURBANCE ($P=1.0\text{PU}, Q=0.2087\text{PU}, X_E=0.4\text{PU}$)

The large signal analysis is carried out by creating a three phase fault at the generator terminal and the fault is cleared after three cycles. Figure 15 and Figure 16 show the system response for

large perturbation with system nominal operating condition. Figure 17 shows the variation in modulating signal for both types of PSS for large disturbance. It is seen from the simulation results that with PSS the system is stable and oscillations die down faster with speed input PSS comparatively. Similarly Figure 18 and Figure 19 show the variation in the rotor angle and power at generator bus for small perturbation with system operating condition $P=0.5$ pu, $Q=0.05$ pu and $x_e=0.2$ pu. Figure 20 and Figure 21 show the variation in the rotor angle and power at generator bus for large perturbation with system operating condition $P=1.2$ pu, $Q=0.65$ pu and $x_e=0.7$ pu.

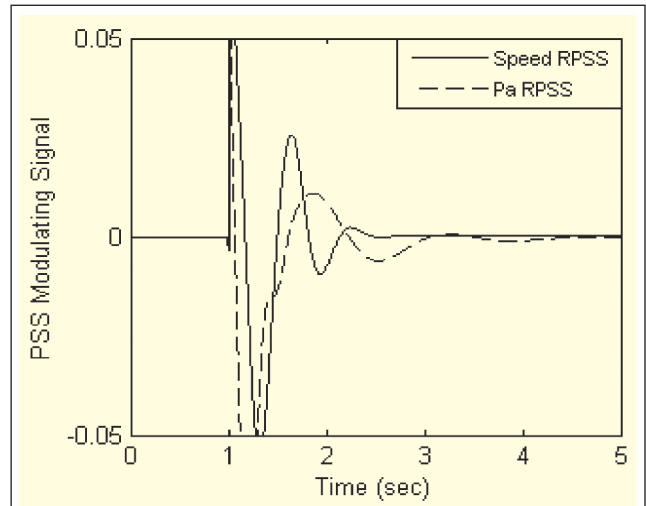


FIG. 17 PSS MODULATING SIGNAL FOR LARGE DISTURBANCE ($P=1.0$ PU, $Q=0.2087$ PU, $X_E=0.4$ PU)

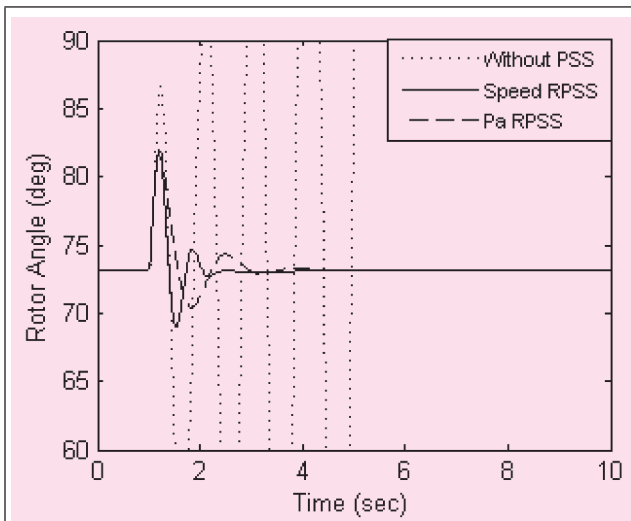


FIG. 15 VARIATION OF ROTOR ANGLE FOR LARGE DISTURBANCE ($P=1.0$ PU, $Q=0.2087$ PU, $X_E=0.4$ PU)

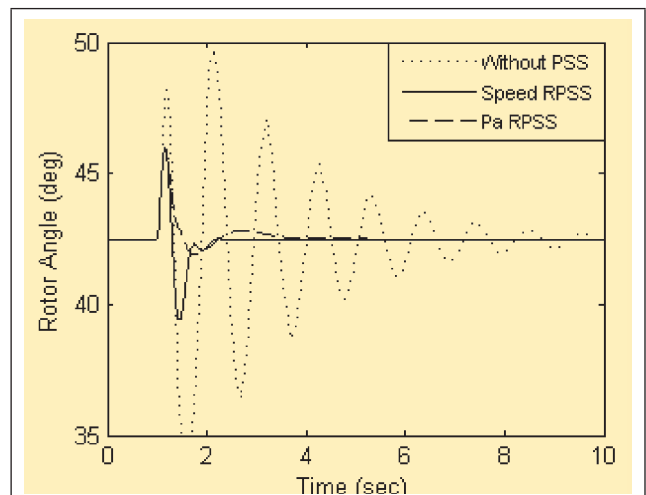


FIG. 18 VARIATION OF ROTOR ANGLE FOR LARGE DISTURBANCE ($P=0.5$ PU, $Q=0.025$ PU, $X_E=0.2$ PU)

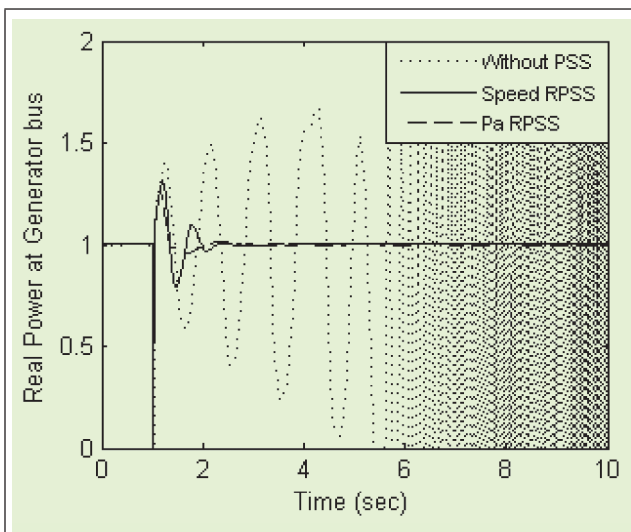


FIG. 16 VARIATION IN REAL POWER AT GENERATOR BUS FOR LARGE DISTURBANCE ($P=1.0$ PU, $Q=0.2087$ PU, $X_E=0.4$ PU)

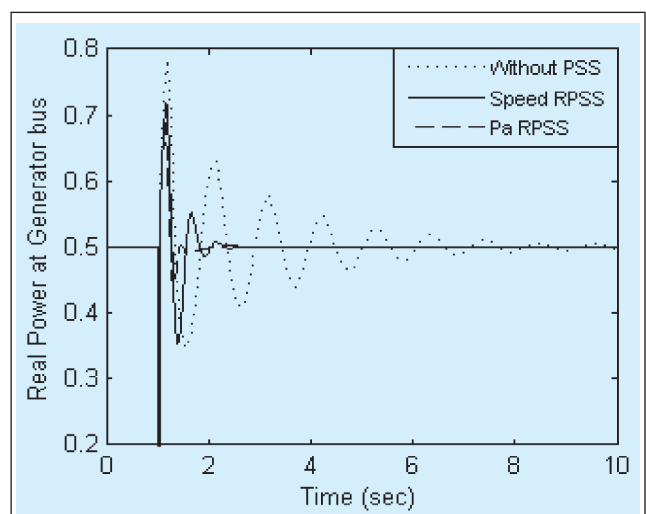


FIG. 19 VARIATION IN REAL POWER AT GENERATOR BUS FOR LARGE DISTURBANCE ($P=0.5$ PU, $Q=0.025$ PU, $X_E=0.2$ PU)

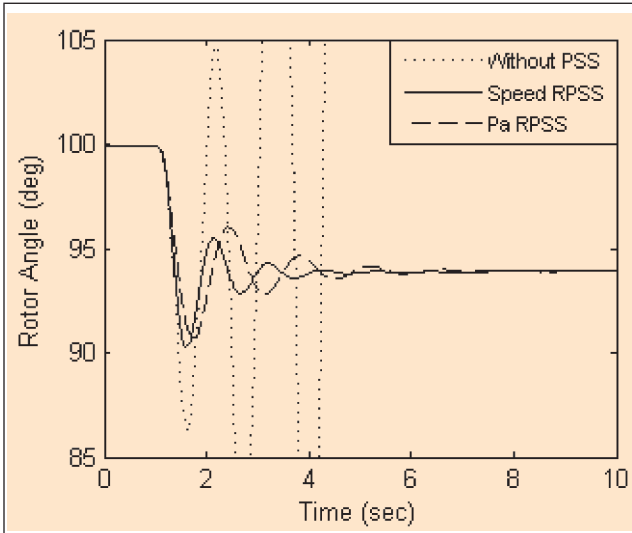


FIG. 20 VARIATION OF ROTOR ANGLE FOR SMALL DISTURBANCE (P=1.2PU, Q=0.65PU, $X_E=0.7PU$)

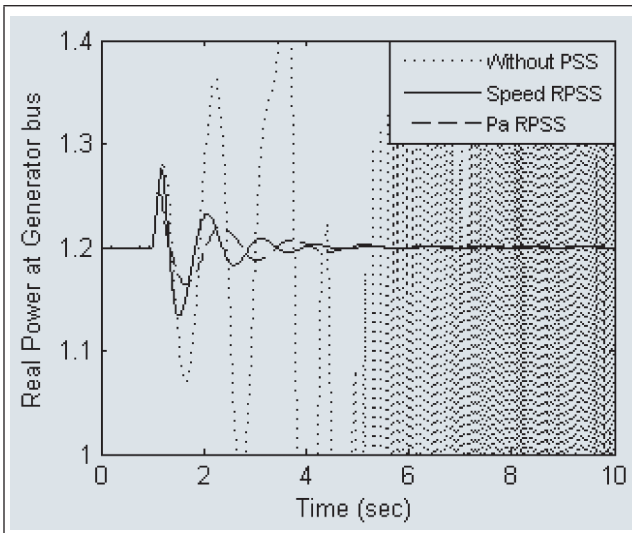


FIG. 21 VARIATION IN REAL POWER AT GENERATOR BUS FOR SMALL DISTURBANCE (P=1.2PU, Q=0.65PU, $X_E=0.7PU$)

9. CONCLUSIONS

The method presented in this paper for designing the accelerating power input and speed input robust PSS is found to be very effective in damping low frequency oscillations arising out of small and large disturbances. The performance requirements in the design of PSS as stated have been achieved. It has been shown that the designed PSSs meet design specifications over a wide range of operating system conditions. The PSS is validated by performing nonlinear simulations

for small and large disturbances. It is found that the damping of oscillations is faster with speed input robust PSS than with accelerating power input robust PSS.

APPENDIX

The generator is modeled as a fourth order system and the SSSC is modeled as a first order system [8].

Generator data:

$$x_d = 1.6, x_q = 1.55, x'_d = 0.32, T'_{do} = 6.0, H = 5.0$$

$$f_B = 60Hz, P = 1.0, E_b = 1.0$$

Transmission and Exciter data:

$$x_e = 0.4, K_e = 200, T_e = 0.05$$

System Simulation Equations:

$$\frac{d\delta}{dt} = \omega_B(S_m - S_{mo})$$

$$\frac{dS_m}{dt} = \frac{1}{2H} [-D(S_m - S_{mo}) + T_m - T_e]$$

$$\frac{dE'_q}{dt} = \frac{1}{T'_{do}} [-E'_q + (x_d - x'_d)i_d + E_{fd}]$$

$$\frac{dE'_{fd}}{dt} = \frac{1}{T_E} [(V_{ref} - V)K_E - E_{fd}]$$

$$T_e = E'_d i_d + E'_q i_q + (x'_d - x'_q) i_d i_q$$

REFERENCES

- [1] I Ngamroo, W Kongprawechnon, "A robust controller design of SSSC for stabilization of frequency oscillations in interconnected power systems", *Electric Power Systems Research* 67 (2003), pp. 161- 176.
- [2] E V Larsen and D A Swann, "Applying Power System Stabilizers Part II: Performance Objectives and Tuning Concepts", *IEEE Transactions on Power Systems*, pp. 3025, June 1981.
- [3] E V Larsen and D A Swann, "Applying Power System Stabilizers Part III: Practical Considerations", *IEEE Transactions on Power Systems*, pp. 3034, June 1981.
- [4] F P de Mello, L N Hannett, J M Undrill, "Practical Approaches to Supplementary Stabilizing from Accelerating Power", *IEEE Transactions on Power Apparatus and Systems*, Vol. PAS-97, No. 5, Sept/Oct 1978.
- [5] Prabha Kundur, "Power system Stability and control", EPRI, McGraw-hill Publication.
- [6] P Shrikant Rao and Indraneel Sen, "A QFT Based Robust SVC Controller For Improving The Dynamic Stability Of Power Systems", *Proceedings of the 4th International Conference on Advances in Power System Control, Operation and Management, APSCOM-97*, Hong Kong, November 1997.
- [7] P Shrikant Rao and Indraneel Sen, "Robust Tuning of Power System Stabilizers Using QFT", *IEEE Transactions on Control Systems Technology*, vol. 7, no. 4, July 1999.
- [8] K R Padiyar, "Power Sytem Dynamics – Stability and Control", Second edition, BS Publications.
- [9] Thomas Coleman, Mary Ann Branch and Andrew Grace, *Optimization tool box. For use with Matlab, User's guide Version 2*, Jan 1999.